

8
MASTER

PREPRINT UCRL- 81220

CONF-781143--2

Lawrence Livermore Laboratory

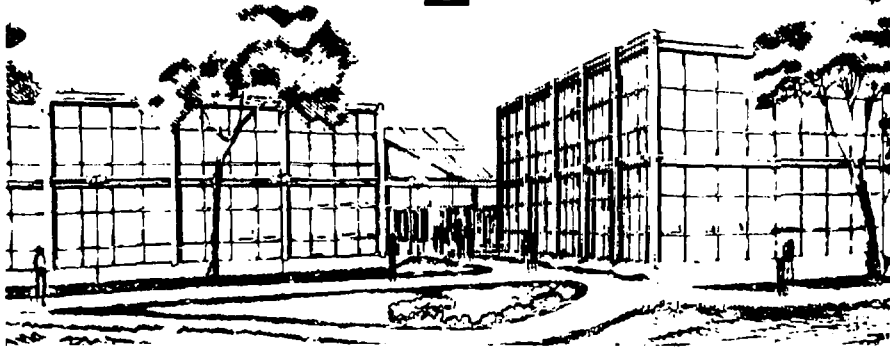
Effects of Various Polishing Media and Techniques
on the Surface Finish and Behavior of Laser Glasses

Richard L. Landingham, Alton W. Casey and Roy O. Lindahl

November 7, 1978

This paper was prepared for presentation at the
American Ceramic Society's Ceramic Machining and
Surface Finishing II, Gaithersburg, Md.,
November 13-15, 1978

This is a preprint of a paper intended for publication in a journal or proceedings. Since changes may be made before publication, this preprint is made available with the understanding that it will not be cited or reproduced without the permission of the author.



DISSEMINATION OF THIS DOCUMENT IS UNLIMITED

ABSTRACT

The advance of high-power laser technology is dependent on the rate of advancement in laser glass forming and surface preparation. The threshold damage of glass surfaces continues to be a weak link in the overall advancement of laser technology. Methods were developed and used in the evaluation of existing glass surface preparation techniques. Modified procedures were evaluated to reduce surface contamination and subsurface defects. Polishing rates were monitored under controlled polishing conditions (purity, pH, particle size distribution, particle concentration etc.). Future work at LLL for this ongoing investigation are described.

"Work performed under the auspices of the
U.S. Department of Energy by the Lawrence
Livermore Laboratory under contract number
W-7405-ENG-48."

... .. (UNCLASSIFIED)
[This report was prepared as a result of work
supported by the U.S. Department of Energy
under contract number W-7405-ENG-48. It
contains information which is classified as
Confidential, Restricted, or Unclassified.
The classification of this report is subject to
the provisions of the Atomic Energy Act of
1954, as amended, and the rules and
regulations of the U.S. Department of Energy.
The report is being made available to the
public in accordance with the provisions of
the Atomic Energy Act of 1954, as amended,
and the rules and regulations of the U.S.
Department of Energy.]

3
fcl

INTRODUCTION

High-power lasers are used to implode D-T targets at LLL. Results from such implosions demonstrate the feasibility of generating electrical power by inertial confinement fusion. The 30-TW SHIVA laser (the world's most powerful laser) was designed and built at LLL for this purpose. This first design used neodymium-doped oxide glass as the amplifying medium. A typical laser chain (50-in long) is shown in Fig. 1. Large increases in laser power are anticipated by using fluoride-base laser glass instead of oxide-base glass in the next upgrade: 200-to 300-TW NOVA solid-state laser design. Such improvements are possible because fluoride amplifiers will have high gain and low nonlinear refraction index. High gain is achieved with optimum balance between emission cross section of the lasing ion and duration of the laser pulse. A smaller cross section is generally needed with increasing pulse width. The emission cross section is host-dependent.

The nonlinear refractive index is most important to the performance of short-pulse high-power lasers. Glasses with low linear refractive index will also have lower nonlinear index coefficients. Glasses with low coefficients propagate laser beams with less distortion. Classes of glasses in order of low index are silicates, phosphates, fluorosilicates, fluorophosphates, and fluorides (BeF_2 is the lowest). The advanced laser designs will need these fluoride glasses, which are now under intense development. Both passive components (lenses and windows) and active components (amplifiers and Faraday-rotation media) of the fluorophosphate glasses (LG-810, E-181, LHG-10, etc.) are being developed commercially for the NOVA design. Scale-up problems similar to those encountered in scaling up the silicate glasses for the large high-power lasers are anticipated.

A more persistent problem common to these glasses is their low resistance to laser damage at their surfaces. This low damage threshold is reduced further when these surfaces are coated. Properly controlled laser damage tests generally confirm that the damage threshold decreases in the following order: bulk glass (highest), bare entry surface, bare exit surface, coated entry surface, and coated exit surface (lowest). Laser pulse duration and wavelength can affect this order.¹ The lower damage threshold of the exit surface as compared to the entrance surface is attributed to a greater optical electric-field strength at the exit surface.² Conflicting results and lack of consistent evidence still prevent adequate explanation of the lower damage threshold for bare and coated surfaces as compared to their bulk glass damage threshold. Surface damage is generally attributed to surface finish and various techniques have been tried to obtain imperfection-free surfaces.³ No improvement in damage threshold is anticipated after achieving surface roughness (rms) of $< 100 \text{ \AA}$.⁴ Surface damage threshold could also be affected by a variety of other surface related features as dust particles, surface films, embedded polishing particles, subsurface scratches and cracks, and residual stresses.⁴⁻⁷

An investigation was initiated this summer at LLNL to evaluate the polishing procedures used to prepare our laser glass components. In this document, we report some of our findings on polishing compounds, subsurface defects, surface chemistry of the polished glass, and techniques developed to evaluate glass surfaces. Since this is an ongoing study, we will also comment on the direction being taken as a result of existing data.

PROCEDURE

This investigation is divided into three parts; (1) evaluation of existing processes, (2) laboratory-scale experiments on modified processes, and

(3) development of techniques to analyze the glasses prepared by these processes. Effort is ongoing in all three areas.

The proprietary nature of most processes used in preparing the surfaces of laser glass hampers our direct correlation of surface conditions with processing stages. The surface conditions from well-established grinding and polishing practices are being evaluated by preparing these surfaces in our Optics Laboratory from glass provided by the laser glass suppliers. Suprasil-II* silica disks (50 mm diam, 10 mm thick) are being evaluated first. The surface damage introduced by coarse grinding and polishing operations is being monitored quantitatively by the Ernsberger technique.⁹ The surface from each state of preparation is polished on cloth laps with fine polishing compound ($< 1 \mu\text{m}$ diam TiO_2) to remove the surface roughness without introducing more deep subsurface defects. Ion exchange or etching techniques are used to expose these subsurface defects and the concentration of defects per mm are determined by image analysis with a Model 720 Imanco image analyzer. Alternate fine polishing and etching steps are used to determine the depth of the defects to within a few micrometers.

The polishing compounds affect the degree of subsurface damage and surface impurity level. The characterization of these compounds includes particle size distribution, surface area, true density, particle shape, phase identification, composition, and impurity level. Impurity levels of other potential contamination sources (carrier solution, anti-foam and dispersion agents, wheel pitch, dressing blocks, etc.) are also checked. The impurity level of the polishing medium is monitored during and after polishing the

* Reference to a company or product name does not imply approval or recommendation of the product by the University of California or the U. S. Department of Energy to the exclusion of others that might be suitable.

glass. The impurity levels of the glass are determined to establish the lowest attainable impurity level on the polished surface.

Several analytical techniques were compared to establish a method of monitoring the surface impurity level after the finer polishing and finishing stages. Ion microprobe, Auger electron spectroscopy (AES), energy dispersive system (EDS), electron spectroscopy for chemical analysis (ESCA), atomic absorption spectrometry, and atomic emission spectroscopy techniques were evaluated.

The characterization of the final surface will include roughness and flatness determinations, laser damage threshold tests, surface impurity analyses, and/or subsurface defect tests. A unique laser damage facility has been developed at LLL to provide rapid and reliable damage threshold results to accelerate the development of laser glass components.¹

We have begun applying some of the experience gained in preparing the Suprasil-II silica surfaces to the preparation of fluorophosphate glasses. The pH level in a high-purity polishing slurry was controlled to determine its effect on polishing rate.

RESULTS AND DISCUSSION

Various final polishing compounds were characterized because most of the contamination and defects on the surface of the glass should come from this final polishing stage (see Table I). The particle size distribution was larger than desired in every case although the mean particle size was $\sim 3 \mu\text{m}$. The large particles were primarily bonded agglomerates, which should break-down if recycled in the final polishing stage. The subsurface damage caused by hard agglomerates is difficult to polish out in this final stage. Neither large single particles nor agglomerates (see Fig. 2) should be present in the final polishing stage. We have removed such particles by three methods: (1) allowing large particles to settle out in a liquid and decanting off smaller particles for polishing, (2) continuous-centrifugation of the polishing solution to remove large particles during polishing and (3) filtering the polishing solution to remove large particles.

No direct correlation between surface area and particle size distribution was observed (see Table I). The surface area of powders is primarily affected by the relatively small amount of fines ($< 1 \mu\text{m}$) in the powder.

The densities of these powders varied both above and below the theoretical density of the supposed major phase. Multiple phases or impurities generally contributed to these types of shifts. Multiple phase compounds make the control of the polishing operation more difficult unless the same ratio of phases can be obtained and behavior of both are understood during polishing operations. Impurities can alter polishing conditions and contaminate the surface of the glass. We determined impurity levels of several compounds being used to polish LLL laser glasses (see Table II). Table II includes impurity levels of two coarser polishing compounds also being used. The impurity levels of other potential sources of contamination are shown in

Table III. These impurity levels should be compared with those in the bulk of the glass (see Table IV) before selecting polishing materials. The impurity levels of all these polishing materials are above those of the bulk glasses so we can expect contamination of the surface and/or difficulty in getting reproducible polishing conditions.

The surfaces of Suprasil-II silica disks were analyzed after final polishing with Liquid 85* by a commercial vendor or with ZOX CE-89 in our Optics Laboratory. Surfaces polished with Liquid 85 were highly contaminated with Ce, Pb, Na, Al, K, and Ca. Trace amounts of Be, B, Mg, Ti, and La were also detected by ion microprobe analyses at depths under the surface of $< 150 \text{ \AA}$. Ion microprobe analysis is not sensitive for P, Sc, and Fe in the presence of Si molecular ions. Auger electron spectroscopy (AES) could only detect C, P, S, Cl, Ca, and N within 10 \AA of the surface. Photoelectron spectroscopy (PES) was able to detect Ce, Sn, Ca, N, and C at the same depth. Trace quantities of Al, Pb, and water were detected at greater depths ($\sim 3200 \text{ \AA}$). As expected, none of these surface impurities could be detected by the energy dispersive system (EDS) in the scanning electron microscope (SEM). Embedded particles of $> 0.1 \mu\text{m}$ could be identified by SEM and analyzed by EDS when exposed at the surface.

The interpretation and turn-around time prevent the use of electron spectroscopy for chemical analysis (ESCA) on routine surfaces. The sensitivity level for several elements of interest is too low to use induction-coupled-plasma (ICP) with direct-reading spectrometry (DRS), flame atomic absorption, or furnace atomic absorption techniques. Evaluation of these surfaces are still in progress by secondary ion mass spectrometry (SIMS).

We have developed a rapid and more quantitative method to detect impurities on these surfaces. We attack teflon fixture to the surface of a glass to contain an etchant ($\sim 2\% \text{ HF}$) within a 13 mm diameter area on the surface. Etchant time and temperature is controlled to dissolve the desired depth of

* Reference to a company or product name does not imply approval or recommendations of the product by the University of California or the U. S. Department of Energy to the exclusion of others that might be suitable.

glass ($\sim 3000 \text{ \AA}$) for subsequent analysis. The actual etch-out depth is profiled with a Det Tak surface analyzer (background threshold of approximately 200 \AA). The solution of dissolved glass is evaporated and analyzed by emission spectroscopy. Three surfaces polished with ZOX CE 89 were analyzed by etching to depths of 1200, 2000, and 2600 \AA , respectively. Surface impurities detected by this method include Na, Al, Ca, Cu, Mg, Fe, Ti, Ba, Ni, Pb, Cr, Mn, Sr, Zr, and Zn. No Ce was detected although CeO_2 was used to final polish these surfaces. This analytical method is not as sensitive to Ce on the ion microprobe method. The bulk glass is contaminated with Al. Additional analyses and development of standards are in progress to improve the accuracy of this method.

A second feature of the above method is that the etched region can be examined optically. Surface and near-surface flaws are revealed by etching or ion exchange techniques.⁹ The deep microcracks caused by rough surface removal operations (blanchard grinding, diamond saw cuts, etc.) have patterns similar to those in Fig. 3. The shallow defects of the coarser polishing operations (30 and $9 \mu\text{m Al}_2\text{O}_3$ polish) used to remove the previous defects are shown in Fig. 4. If proper amounts of the surface are removed during each stage of polishing, these deep defects will not be observed after etching a surface polished with fine ($\leq 1 \mu\text{m}$) polishing compounds. Etching such a finely polished surface does expose the polish scratches previously filled in and/or covered over by a surface film (see Fig. 5). The concentration of scratches and defects can be determined by image analysis and compared with laser damage results to establish a quantitative correlation. Such information would be useful in establishing inspection limits on surfaces before coating or bare-surface use.

The laboratory scale polishing unit (305 mm diam wheel) was set up to final polish the Suprasil-II silica disks with high-purity polishing slurries. We stopped using pitch on this wheel after we observed that the pitch reacted with the polishing slurry and was picked up on the glass. Nylon covered wheels allowed better monitoring of polishing rates and impurity levels. Evaluation of surfaces suitable for commercial polishing applications will be investigated after the questions about impurity effects have been resolved.

The characterization results are given in Table V and VI for the high-purity powders used on the laboratory-scale polishing studies. These powders were used on the final polishing stage to remove the defects of the two previous coarse stages (Al_2O_3 microgrit 300 and 9% in Table II). To date, we have polished Suprasil-II silica disks (51 mm diam) with MgO , CeO_2 (B-1407), and both Al_2O_3 powder and a fluorophosphate glass (ZG-812) disk (25 mm diam) with the ZnO powder. The adjusted polishing parameters and polishing rates for these initial studies are listed in Table VII. Polishing with MgO was discontinued because additives would be required to control excessive foaming. High polishing rates with CeO_2 powder were obtained after the coarse particles ($> 5 \mu\text{m}$ diam) were removed while maintaining a constant concentration of particles ($< 5 \mu\text{m}$ diam) in the polishing slurry.

Polishing with Al_2O_3 (ERC-HP-DBR) powder was stopped because of excessive foaming. This foaming action was attributed to the Mg doping agent in this hot press powder. Satisfactory polishing rates were obtained with the Al_2O_3 (4071) powder, but subsurface scratches persisted after 35 h of polishing with the same slurry. Starting with a finer agglomerate size ($< 5 \mu\text{m}$ diam) Al_2O_3 slurry and continuously removing large agglomerates ($> 5 \mu\text{m}$ diam) from the slurry reduced subsurface scratches. Preliminary evidence indicates a rapid buildup (snowballing) of agglomerates comprised of Al_2O_3 particles.

and silica from the glass (see Fig. 6). This buildup was also observed by determining the particle distribution size of the slurry before and after polishing. Further evaluation of this buildup mechanism is in progress because it could account for the common belief that Al_2O_3 is "too hard" to polish glass.

Our first attempt to polish fluorophosphate glass was made with ZnO (8832) powder with controlled pH slurry (see Table VII). At lower pH values (< 7.0), the foaming was not excessive, and a maximum polishing rate was observed at 6.5 pH. Fewer subsurface scratches were observed with ZnO on the fluorophosphate glass than observed with Al_2O_3 on the silica glass. Additional polishing studies are in progress on both glasses.

Laser damage tests have begun to establish the threshold damage of Suprasil-II silica surfaces after various polishing and etching procedures. A separate report will be prepared when we have sufficient results to show a direct relationship between specific impurity levels, defects, and surface threshold damage.

CONCLUSIONS AND RECOMMENDATIONS

The rapid advance of high-power lasers for fusion applications requires advances in glass fabrication, glass surface preparation, and glass coating techniques, to sustain laser stability and durability. Since the laser threshold damage of glasses seems to be the weakest link, we examined existing surface preparation procedures as well as evaluated alternate methods to reduce surface contamination and subsurface defects. Analytical techniques were developed to quantitatively determine surface impurities and subsurface defects. The origin of many of these impurities and defects were identified.

Closer control of final polishing compounds is needed to assist opticians in meeting the increasing constraints on surface finishes. Characterization of polishing compounds should at least include impurity content, phase content, particle size distribution, and nature of large particles and/or agglomerates. Such information could prevent problems in subsequent polishing operations, which might trigger unwanted changes in those procedures.

The contamination of the polished surface by the polishing slurry has been confirmed. Efforts to maintain a low contamination level in this slurry should improve polishing operations as well as laser threshold damage. The chemical reactions at the glass-slurry interface seem to control polishing rates as well as polishing particle breakdown or growth (snowballing) rates. More work in this area is in progress at LLL.

ACKNOWLEDGEMENTS

This investigation was initiated and supported by Norman Brown of the Optics Laboratory and Howard Lowdermilk and Lee Smith of the Laser Damage Group at LLL. Their assistance and guidance made this report possible. Dave Milam of the Laser Damage Group has been most helpful in directing us in matters relating to and evaluation of laser damage tests. Al Ulrich has prepared and evaluated many of the glass surfaces by metallographic techniques. Charlie Farrell developed the procedures used to detect impurities and defects on the surface of these glasses. The unique support of Carol Weaver and Chuck Slettevold was needed in the characterization of all the polishing compounds.

REFERENCES

1. Milam, D., "Laser-induced Damage at 1064 nm, 125 psec", *Applied Optics*, Vol. 16, May 1977, pp. 1204-1213.
2. Crisp, M. D., Boling, N. L., and Dube, G., "Importance of Fresnel Reflections in Laser Surface Damage of Transparent Dielectrics", *Appl. Phys. Lett.*, Vol. 21, No. 8, October 15, 1972, pp. 364-366.
3. Fradin, D. W. and Bass, M., "Comparison of Laser-Induced Surface and Bulk Damage", *Appl. Phys. Lett.* Vol. 22, No. 4, February 15, 1973, pp. 157-159.
4. Milam, D., Smith, W. L., Weber, M. J., Genter, A. H., House, R. A., and Bettis, J. R., "The Effects of Surface Roughness on 1064-nm, 150 ps Laser Damage", in Laser Induced Damage in Optical Materials: 1977, A. J. Glass and A. H. Guenther, eds., Nat. Bur. Stand. (U.S.) Spec. Publ. 509, pp. 166-173.
5. House, R. A., Guenther, A. H., and Bennett, J. M., "Surface Roughness Statistics of Fused Silica as a Function of Surface Preparation and Treatment", in Laser Induced Damage in Optical Materials: 1977, A. J. Glass and A. H. Guenther, eds. Nat. Bur. Stand. (U.S.) Spec. Publ. 509, pp. 157-165.
6. Bloembergen, N., "Role of Cracks, Pores, and Absorbing Inclusions on Laser Induced Damage Threshold at Surfaces of Transparent Dielectrics", *Applied Optics*, Vol. 12, No. 4, April, 1973, pp. 661-664.
7. Ringlien, J. A., Boling, N. L., and Dube, G., "An Acid Treatment for Raising the Surface Damage Threshold of Laser Glass", *Applied Physics Letter*, Vol. 25, No. 10, November 25, 1974, pp. 598-600.
8. Boling, N. L., Ringlien, J. A., and Dube, G., "Q-Switched Laser Induced Surface Damage at 1.06 Microns", in Laser Induced Damage in Optical Materials: 1974", edited by A. J. Glass and A. H. Guenther, Nat. Bur. Stand. (U.S.) Spec. Publ. 414, December, 1974, pp. 119-130.
9. Ernsberger, F. M., "Origin and Detection of Microflows in Glass", Fracture Mechanics of Ceramics, Volume 1, Concepts, Flaws, and Fractography, edited by R. C. Bradt, Plenum Press, N.Y. - London, 1974.

NOTE

This report was prepared as a result of work sponsored by the United States Government. Neither the United States nor the United States Atomic Energy Commission, nor any of their employees, nor any of their contractors, subcontractors, or their employees, makes any warranty, express or implied, or assumes any legal liability or responsibility for the accuracy, completeness, or usefulness of any information, apparatus, product, or process disclosed, or represents that its use would not infringe privately-owned rights.

Reference to a company or product names does not imply approval or recommendation of the product by the University of California or the U. S. Department of Energy to the exclusion of others that may be suitable.

TABLE I. Glass Polishing Compounds.

Compound	Density, g/cm ³	Phases detected by x-ray diffraction	m ² /g	X-ray fluorescence	Particle size range, μm	Status ^a of large particles
MgO (Code 920)	3.58	Cubic + unident Lines	26.84		0.01-15	S
SnO (AV-116)	6.45	Tetrga SnO ₂ + Sn ₃ O ₄	11.27		0.01-10	A
ZnO (HSA)	4.84	Hexag. + unident lines	50.79		0.01-30	A
TK68	6.77	Ce ₆ WO ₁₂ Type ^b	2.82	Ce(s),La(s),W(vvw)	0.03-10	A
Rhodite 15	6.20	CeO ₂ (s) CeOF(w)	3.42		0.01-15	A
Rhodite 50	5.91	CeO ₂ (s) CeF ₃ (w)	12.49	Ce(s),Ca(m),W(vvw)	0.01-20	S
Rhodite 76	6.38	CeO ₂ (s) CeOF(w)	6.21		0.01-20	A
ZOX CE89	6.05	Ce ₆ WO ₁₂ Type ^b	16.36		0.01-10	A
ZOX E	5.78	ZrO ₂ ¹	14.59		0.01-10	A
Cerium 85	6.603	Ce ₆ WO ₁₂ (s) Type ^b + CeCO ₃ F(w)	29.01	Ce(s),La(s),W(vvw)	0.01-7	A
Lustrox 1200	4.97	ZrO ₂ (s) ^d + ZrO ₂ (w) ^c	20.32	Zr(s)	0.01-12	A
Lustrox PG	3.41	ZrO ₂ ^c	27.78	Zr(s)	0.01-20	A
ZnO ^e	5.61	Hexag. (5-660)	7.18		0.02-15	A

^a S = single particle and A = agglomerate particle.

^b Ce₆WO₁₂ crystal type structure but La replaces W.

^c (13-307) ZrO₂ monoclinic (variable brown to colorless) Baddeleyite.

^d (14-534) ZrO₂ Tetragonal.

^e Reagent grade powder (8832).

TABLE II. Impurities in polishing compounds as determined by emission spectrometry.

Impurity elements	Impurity levels in polishing compounds, ^a ppm						Reagent grade ZnO
	MgO Code 920	SnO AV-116	Liquid 85 ^b	ZOX CE-89	Al ₂ O ₃ Microgrit 30T	Al ₂ O ₃ Microgrit 9T	
Al	300	<5000	nd	nd	major	major	<100
Cu	6	1	10	10	4	nd	3
Si	600	1000	nd	nd	1 Wt%	1 Wt%	< 2
Fe	200	600	≥1000	1000	1000	1000	nd
Ca	3000	100	2000	20	3000	3000	<2
Zn	< 30	100	nd	<1	< 30	<30	major
Ni	10	60	nd	< 1	5	5	<3
Cr	<10	30	nd	1000	< 10	<10	<10
Ag	<1	<1	nd	nd	<1	3	<1
Sr	10	<1	≥1000	1000	100	1000	<1
V	<10	<10	nd	nd	40	20	< 30
Pb	<10	<10	600	60	< 30	< 30	<10
La	nd	nd	nd	≥10 Wt%	nd	nd	nd
Ba	<100	<10	≥1 Wt%	5000	< 30	< 30	<100
Nb	< 30	<30	≥1000	300	< 30	< 30	<100
Mn	10	<1	30	20	5	5	<10
Mg	nd	nd	≥1000	10	500	500	<1
Na	< 300	nd	100	3000	3000	nd	nd
Ti	10	nd	nd	800	800	nd	<10
Ga	nd	nd	nd	30	30	nd	nd
Zr	<10	nd	≥1000	nd	nd	nd	nd

^a nd means not detected.

^b Y and Th level at 100-1000 according to x-ray fluorescence.

Table III. Other sources of contamination during laser glass polishing operation.

Impurity elements	No. 64°C melt	Pitch 73°C melt	82°C melt	Ever-Flo Solution
Al	3	2	2	1
Cu	0.1	0.1	0.1	<1
Si	10	2	2	2
Fe	3	10(60) ^a	7	1
Ca	3	1	2	2
Zn	<1	<1(5) ^a	7	<1
Ni	7	6(10) ^a	2	<1
V	10	10(20) ^a	7	<1
Pb	<1	<1(5) ^a	<1	2
Mg	1	0.6	0.7	<2
Na	<6	<6	<6	25
Ti	2	<0.3	<0.3	<1
K	nd	nd	nd	25

^aX-ray Fluorescence Analysis (xx)

(Note: nd means element was not detected)

TABLE IV. Impurities in laser glasses as determined by emission spectrometry^a

Impurity elements	Impurities, ppm		
	BK-7	Laser glasses LG-812	ED-2
Mg	100	major	10
Mo	200	2000	1000
Ba	major	1000	60
Si	major	20	major
Cu	3	6	3
Sr	60	major	major
B	major		100
Sn	< 30	< 10	30
Ti	200	< 10	< 3
As	1000	< 30	300

^a Major = additives or major elements of glass composition; blanks mean not detected

TABLE V. Material characterization of high-purity powders under evaluation as polishing compounds.

Powder type	Density, g/cm ³	Phases detected by x-ray diff.	Surface area, (m ² /2)	Particle size ranges, μm	Status of large particles ^a
AnO (Code 8832)	5.61	Hexag.	7.2	.02-15	A
MgO(100m)	3.58	Cubic + Moderate Mg(OH) ₂	76.6	.01-25	A
CeO ₂ B-1407	7.03	F.C.C.	1.4	.05-20	A
CeO ₂ B-1408	7.09	F.C.C.	1.2	.05-20	A
CeO ₂ B-1409	7.58 ^b	F.C.C.	6.6	.05-25	A
Al ₂ O ₃ ERC	3.97	Alpha Al ₂ O ₃ +Unknown lines	7.4	.03-20	A
Al ₂ O ₃ Lot 4071	3.93	Alpha Al ₂ O ₃ +Unknown lines	9.6	.03-18	A

^a S = single particle, and A = agglomerate.

^b After vacuum bakeout at 230°C this density dropped to 7.13 g/cm³, but the particle size range remained the same.

*** Unknown = unknown lines also detected.

TABLE VI. Impurities in high-purity powders under evaluation as polishing compounds as determined by emission spectrometry)^a

Impurity elements	Impurities, ppm						
	ZnO 8832	MgO 100m	CeO ₂ B-1407	CeO ₂ B1408	CeO ₂ B-1409	Al ₂ O ₃ ERC-HP- DBM	Al ₂ O ₃ 407I
Cu	3	10	≤10	nd	nd	4	1
Mg	<1	nd	6	6	≤ 2	100	100
Si	<2	100	nd	nd	nd	110	100
Ca	<2	3000	1000	nd	nd	25	30
Fe	<10	300	15	< 5	≤ 5	30	30
Ga	nd	<3	nd	nd	nd	100	20
Mn	<10	30	10	≤1	nd	<1	3
B	<3	300	100	nd	nd	<3	<3
Ba	<100	<100	100	nd	nd	<30	nd
Pb	<10	<10	2	2	2	<30	<30
Al	nd	200	nd	nd	nd	major	major
Sr	nd	30	nd	nd	nd	<1	nd

^a nd mean not detected.

TABLE VII. Results vs adjusted parameters of laboratory scale polishing with high purity powders.

Polishing compound	Polishing pH*	Polishing time, h	Glass Removal Rate		Remarks
			Wt, g/h	Thickness, $\mu\text{m}/\text{h}$	
MgO (100m)	9.8-9.7	27.5	250	0.11	Excessive Foaming
CeO ₂ (B-1407) as received	8.3-6.8	27.5	990	0.44	
CeO ₂ (B-1407) as received	6.8-7.2	27.5	3,900	0.48	Control pH
CeO ₂ (B-1407) -5 μm fraction	8.9-7.5	34.5	4,600	2.06	
Al ₂ O ₃ ERC HP-DBM	8.0-7.7	17.5	1,800	0.82	Excessive foaming
Al ₂ O ₃ (4071) as received	9.0-7.9	35	1,600	0.71	
Al ₂ O ₃ (4071) -5 μm fraction	8.3-7.4	24.5	760	0.34	Decreasing Al ₂ O ₃ conc. (50%) due to decant of large particles (>5 μm dia).
ZnO (8832) as received	5.9-5.8	13	420	1.80	Control pH
ZnO (8832) as received	6.5-6.6	13	780	3.32	Control pH
AnO (8832) as received	9.0-8.5	13	500	2.15	Control pH. Excessive foaming.

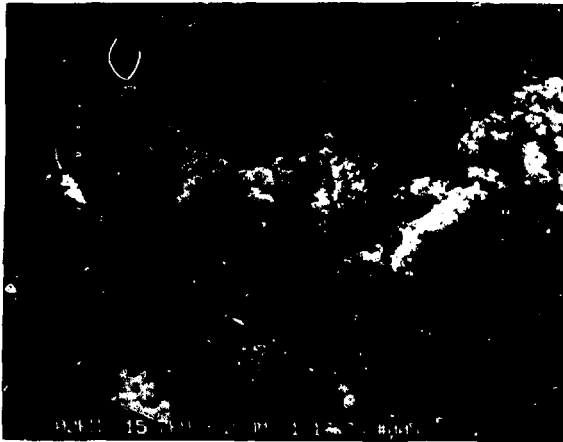
* pH values before and after polishing



Fig. 1 The installation of components in the Shiva laser system at the Lawrence Livermore Laboratory.



a. Single large particles in MgO (Code 920).



b. Large agglomerate particles in SNO(AV-116)

Fig. 2. Photomicrograph of typical large particles discovered in final polishing compounds by scanning electron microscopy.



as-polished

etched

a. Defect pattern in diamond saw cut surface

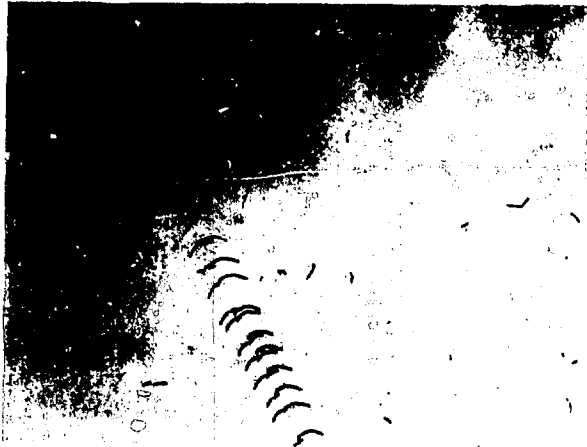


as-polished

etched

b. Defects patterns in blanchard ground surface

Fig. 3. Surface defects revealed on Suprasil-II silica surfaces after etching with HF(10DX).

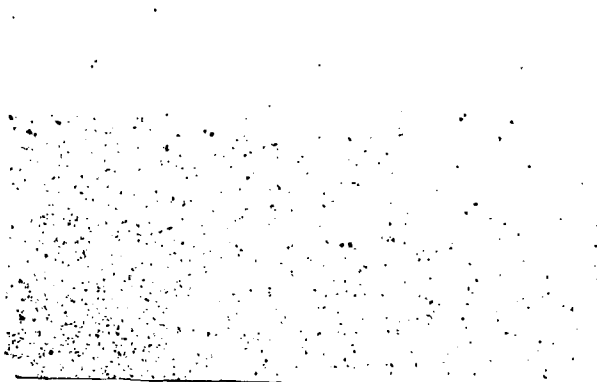


as-polished

etched

100X

a. Coarse polish with $30 \mu\text{m Al}_2\text{O}_3$ compounds



as-polished

etched

100X

b. Coarse polished with $9 \mu\text{m Al}_2\text{O}_3$ compound

Fig. 4. Surface defects revealed on Suprasil-II silica surface after etching with HF

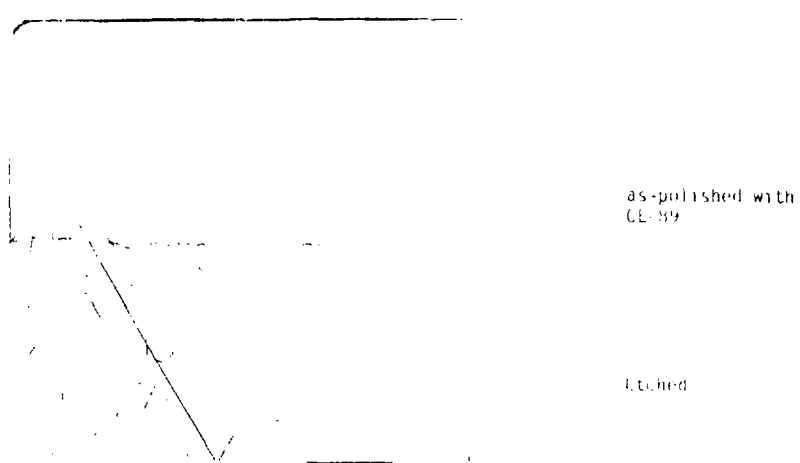


Fig. 5. Surface scratches on Suprasil-II silica are apparent after etching with HF.

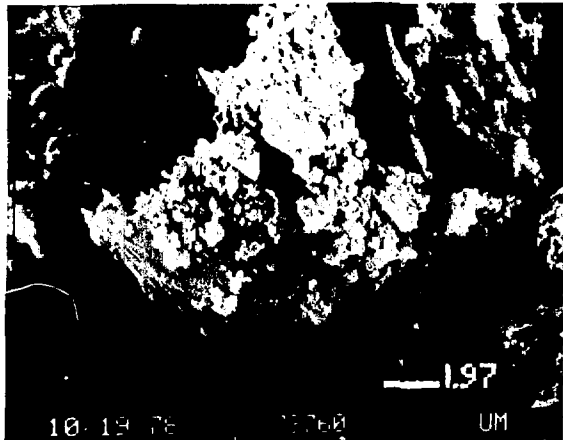


Fig. 6. Buildup (Snowballing) of large agglomerates in the final polishing slurry were photographed (above) in the SEM and analyzed by EDS. These agglomerates were made up of aluminum, silicon, and oxygen and formed during final polish of silica glass with Al_2O_3 polishing compounds.